SINGLE-STEP, REDUCED SHEAR, MICROFLUIDIC EXTRUSION OF BLOOD BRAIN BARRIER

by

Isaac Henderson Wetzel

A thesis submitted to the faculty of
The University of North Carolina at Charlotte
In partial fulfillment of the requirements
For the degree of Master of Science in
Mechanical Engineering

Charlotte

2019

Approved by:

_____
Dr. Hansang Cho

_____
Dr. Mark Clemens

_____
Dr. Charles Lee

_____
Dr. Didier Dréau

_____
Dr. Ian Marriot

ABSTRACT

ISAAC HENDERSON WETZEL. Single-Step, Reduced Shear, Microfluidic Extrusion of Blood Brain Barrier. (Under the direction of Dr. HANSANG CHO)

Three-dimensional (3D) bioprinting of living structures with cell-laden biomaterials has been achieved in vitro, however, central nervous system tissues have been limited by the low viability printing of cerebral vessels, using conventional printing processes. To create a more viable cerebral vessel, reduced shear stress, multicellular, heterogeneous, perfusable blood brain barrier, a microfluidic print head and bioink was designed. Comsol simulations were used to map the theoretical flow profile of different microgroove structures to facilitate the design of a microfluidic print head. The print head was fabricated via standard SU-8 protocols and consisted of two A- symmetrically aligned PDMS pieces. To create a more viable and printable bio-ink, sodium alginate was mixed with highly concentrated collagen (35mg/ml) to form a cell friendly bio-ink. To confirm viability of the bioink and printing process, promodium iodide and nucleus dye were used on 2D disks. Endothelial cell attachment was observed 24 hours after plating. The 2D disk showed high viability of 97 ± 3% after 3 weeks of culture. In conclusion, microfluidic print head design simulation was capable of producing 3D hydrodynamic focusing of water. The bioink was capable of 2D printing process and producing a highly viable endothelial cell pallet. The microfluidic print head and bioink could be used in unison for future bio printing systems to quickly print vessels with smaller size or have the addition of the different cell types to create a neurovascular unit.

ACKNOWLEDGEMENTS

I would like to acknowledge Eric Cutler for his contribution to the Comsol simulation. I would also like to acknowledge Wil Groves, Dr. Yojoung Kang, and Dr. Joseph Park for their valuable input resulting in multiple hydrogel candidates. Special thanks to UNC Charlotte for providing the facilities and program. Thanks to family and friends for their continued support through my graduate degree. Finally, I'd like to thank Dr. Hansang Cho for his financial support and years of mentorship.

TABLE OF CONTENTS

LIST OF FIGURES

CHAPTER 1: INTRODUCTION

Today 1/6 people suffer from a neurovascular condition[1]. The blood brain barrier is the base to understanding these neurological disorders. Current models are limited to animal and simple in-vitro models that may express different therapeutic and pathological outcomes[1]. Therefore, there is a need for a new model capable of reproducing the neurovascular unit. This project focuses on creating a more physiological blood brain barrier by improving current bio-printing techniques.

Three dimensional (3D) multicellular models and complex tissues depend on the microcirculation of nutrients and oxygen through their vascular structure to retain viability. Due to the complex nature of current 3D vessel fabrication in tissues, bio printing has emerged as an attractive method for engineering 3D tubular networks. In 3D bio printing, layer-by-layer precise positioning of biological materials, biochemical and living cells, with spatial control of the placement of functional components, is used to fabricate 3D structures.

The three main printing technologies used for deposition and patterning biological materials are inkjet[20,21,22,23], micro extrusion[28,29,30,31,32], and laser assisted printing[18,19,24,25,26,27]. Inkjet printers deposit controlled volumes of biomaterials by electrically producing droplets in predefined locations. The significant disadvantages of this technology is the requirement of the biomaterial to be in liquid form for droplet formation and then be cured to support a 3D structure, and the risk of mechanical and thermal stresses on the biological materials. Micro extrusion printers function by robotically controlling a micro extrusion print head and stage that layer needle extruded filaments into a 3D structure. The significant disadvantage of this technology is the

difficulty to achieve both high cell viability and at high resolutions due to the tradeoff between needle diameter, which controls resolution, and shear stress induced on cells during extrusion, which increases with smaller diameter needles. Laser-assisted bio printing functions using focused laser pulses on an absorbing layer of the ribbon to generate a high-pressure bubble that propels cell-containing materials toward a collector substrate. The major limitations of this technology is lead time to create ribbon substrate, metallic residue left on cell substrate after printing, and cost of laser machine.

From these basic printing technologies, coaxial printing has emerged. Originally coaxial printing was an electrospinning technique in which two immiscible liquids are electrospinned through a coaxial, two-capillary spinneret to fabricate several kinds of hollow nano-filaments. It has now recently been successfully adopted in tissue engineering[35] Ibrahim T Ozbolat and workers[36] have explored the characteristics of the channels fabricated with a coaxial nozzle. They designed a pressure-assisted freeform fabrication platform combined with a coaxial nozzle dispenser unit to print hollow filaments based on the gelation process of sodium alginate and calcium chloride solution. Then they investigated the dehydration, swelling, degradation, per fusional, permeable, and mechanical properties of the printed microfluidic channels[37,38,39]. In another report, they designed a multi-arm bio-printer with two nozzles mounted on independent arms to concurrently print a filament structure and deposit cell spheroids between the filaments to create a hybrid structure to support the cell spheroids in three dimensions[40]. Their work presented a very useful method to fabricate fluidic microchannel as an alternative to biometrically fabricated bifurcated vessels or microfluidic vessels. From these early studies, groups have printed cell laden tubular structures to recreate implantable veins and

arteries [41,42,42]. Coaxial printing has shown great promise, however it is significantly limited by wall thickness and vessel diameter. Due to the machining limitations of stainless steel needles, vessel wall thickness can reach a minimum of 50 um and diameters 500 um, while increasing shear stress. These limitations further increases the chances of multilayered endothelium, non-physiologically relevant models, long maturation time, and reduced viability.

To overcome the machining limitations of coaxial printing, groups have developed microfluidic bio-printing as a way to create more physiologically relevant models[47,48,49]. Using the spatial control of microfluidic flow generators as a base[6,7,8], groups have successfully patterned many different types of fibers, including tubular[48]. The use of microfluidic print heads significantly reduce the amount of hydrogel used, reducing the price of expensive hydrogel, reagents, and number of cells. Furthermore, the direct control over cell patterning and control of extrusion speed add an extra dimension. Still the patterns created are simple including rectangle, simple sheath, or dual hemisphere[49]. Additionally, they produce large amounts of shear stress due to the low diameters.

In addition to bio-printing strategies limiting the capability of a physiologically relevant neurovascular model, the relevant selection of hydrogel must also be discussed. In bio printing, hydrogels as cell delivery vehicles. Many types of cells can be viable when encapsulated within hydrogels, such as fibroblasts, chondrocytes, hepatocytes, endothelial cells, adipocytes, and stem cells[13]. During bio printing, a hydrogel with suspended cells is processed into a specifically defined shape, which is successively fixed by gelation. Gelation is usually a crosslinking reaction initiated by physical, chemical or a combination of both processes. Physical crosslinking is a reversible interaction that depends on meshes

of high molecular polymer chains, ionic interactions and hydrogen bridges[14]. This type of crosslinking is compatible with biological systems such as growth factors and living cells. However, poor mechanical properties are considered as the main drawback of physical crosslinking reaction. Therefore, post processing crosslinking and/or an additional crosslinking agent is required. One example of chemical gelation by interaction between anionic groups on alginate (COO) with divalent metal ions (Ca2+). In contrast, chemical crosslinking forms new covalent bonds, which give relatively high mechanically stable constructs compared to physical crosslinking[14]. However, this type of crosslinking may involve exposure of constructs to toxic ionic solutions.

A few more examples of viable hydrogels are alginate[44], gelatin methacryloyl (GelMA)[45], and photocurable hyaluronic acid[46]. However, these hydrogels usually suffer from low cellular affinity (e.g., alginate) or strong stiffness (GelMA)[47]. Consequently, the limited cell activity impeded the development of a functional vascular model. Moreover, the lack of a platform providing consistent and tunable perfusions to the delicate hydrogel conduits hampered the integration of mechanical and biochemical signals for biomedical applications.

CHAPTER 2: DESIGN OF MICRO-FLUIDIC PRINT HEAD FOR 35 MICRO-EXTRUSION OF HYDROGEL

In order to overcome the limitation of conventional 3D vessel printing and hydrogels, we propose an adaptable microfluidic print head capable of producing more versatile shapes of 3D vessels, network with highly viability through a single-step microfluidic extrusion. The project will be split into two parts. The first being microfluidic design. The microfluidic print head will induce a 2D focused sheath flow combined with the microextrusion printing strategy to create the lumen in a single step by using a flow generator as a base. The laminar flow characteristics of the two biomaterials combined with the geometric features of the microfluidic chip causes patterning of multiple layers (core, intermediate sheath, outer sheath). The intermediate sheath will be a hydrogel including endothelial cells. The core will contain a crosslinking buffer,that is replaced after extrusion. The outer sheath will be laden with pericytes.

By adjusting the ratio of flow rates between core, outer and intermediate sheaths the layer thickness of each layer can be fine tuned to allow a single layer extrusion of endothelial cells, reducing the maturation time and overcoming the spatial resolution limitation of conventional micro extrusion. As the larger needle diameter is allowed, it will induce lower mechanical shear stresses on the cells during extrusion, thus increasing viability. Therefore, this microfluidic extrusion will achieve both higher viability and high spatial resolution at the same time. Also, after printing the 3D vessels, they will be embedded in a supportive hydrogel and polymerized at a culturing temperature. Meanwhile, a cavity will be created by removing the cross linker from the core with media perfusion.

The chevron geometry generator will be selected as the best candidate for the print head, due to its independence of flow ratios for core focusing. The print head must have the ability to 2D hydrodynamic focus three separate fluids. In addition, it must be able to pattern a 10-25 um thick, uniform intermediate layer for single layer endothelial extrusion. The wafer design of the print head needed to have a way of alignment after device fabrication. Finally, the device needed to have low shear stress during extrusion.

2.1 Material and Methods

Comsol Simulation

Comsol simulation flow dimensions were created using Creo Parametric software to generate .stl of varying parameters, including focal points, depth, width, and length, of chevron geometries. The geometries were imported into Comsol where flowrates for the core, intermediate sheath and outer sheath were varied. The flowrates ranged from 0um/s to 300 um/s. Streamlines were projected and cross section taken throughout the geometry to confirm hydrodynamic focusing. Liquid water was assumed as the model fluid.

Device Fabrication

Negative photoresists, SU-8 50 and SU-8 100 (MicroChem, Newton, MA, USA), were sequentially patterned using standard lithography on a 4'' silicon wafer to create a mold for exrusion migration channels of 75 Um in height and chevron geometry of 25 Um in height. A mixture of a base and a curing agent with a 10:1 weight ratio (SYLGARD 184 A/B, Dow corning, Midland, MI, USA) was poured onto the SU-8 mold and cured for one hour at room temperature under vacuum and, subsequently, cured for more than 3 hours in an oven at 80 °C. The cured poly dimethyl-siloxane (PDMS) replica was peeled off from the mold and holes were punched for inlet reservoirs. Ethanol was applied onto

compartment side of PDMS slab. Both A-symmetrical PDMS slabs were brought together and aligned via large optical course alignment markers located on the sides of the device and fine alignment markers located near the channels. After alignment, the device was heated at 60C to evaporate the ethanol and finalize the bond.

Microfluidic Print Head Design

Micro-fluidic print head was designed via Auto CAD modeling software. The Auto CAD model was exported to Link CAD for mask fabrication.

2.2 Results

Comsol Simulation Results of Chevron Geometry

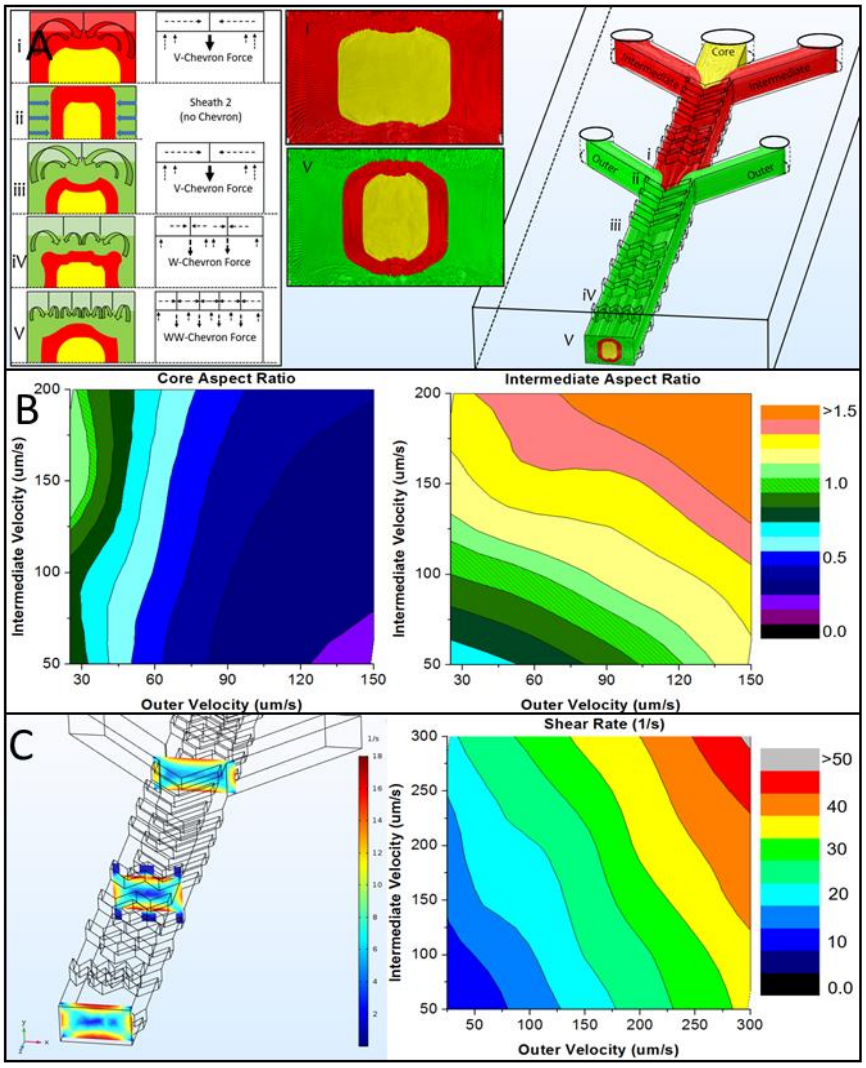

FIGURE 1: Simulation of Micro Fluidic Print Head (a) Effect of chevron geometry of fluidic streamlines. Isometric view and cross sectional view of steam lines. (b) Aspect rations of sheath thickness of core and intermediate sheath thickness.(c) Shear stress analysis

Simulation results confirmed the chevron geometry was adequate in 2D hydrodynamic focusing. Additional forms of chevrons were used including w and ww forms. The additional form dampened the effect of the chevron geometry and allowed for

a higher uniformity of the intermediate sheath (a). The geometry was capable of high uniformity of the intermediate sheath at outer velocity from 60 um/s to 250 um/s and intermediate velocity from 75 um/s to 150 um/s (b). The core was fixed at 50 um/s and showed greatest uniformity at outer sheath 30 um/s to 50 um/s and intermediate velocity of 50 um/s to 200 um/s (b). Shear stress analysis showed a safe cellular extrusion range of 50 um/s to 300 um/s for both the intermediate sheaths and outer sheaths. The core speed was fixed at 50 um/s (c). The cross section at critical point within the geometry showed reduce shear at the critical intermediate sheath as well as, low shear throughout the print head (c).

Wafer Design of Print Head Version One

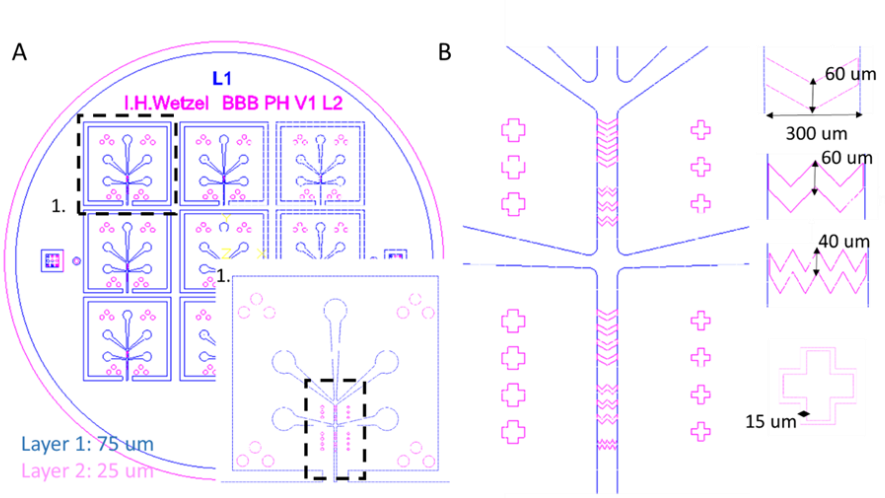

FIGURE 2 CAD Design Of Print Head Version 1 (a) Wafer scale of A-symmetrical device and single device scale. (b) View of chevron geometry and micro channels. Geometry of chevron and micro alignment markers.

Microfluidic print head was designed via Auto Cad software. It is composed of 5 inlets. Inlet one is for core cross linking solution, calcium chloride. Inlet 2 and 3 are for

sheath intermediate, which will consist of endothelial cells. Inlets 4 and 5 are for outer sheath. This sheath will consist of pericyte and other brain cells. The large circles and box frame are for course alignment of PDMS. The small cross symbols are for fine alignment of the structures. The height of layer 1 (blue) is 75 um. The height of the chevron geometry is 25 um.

Wafer Fabrication of Print Head Version One

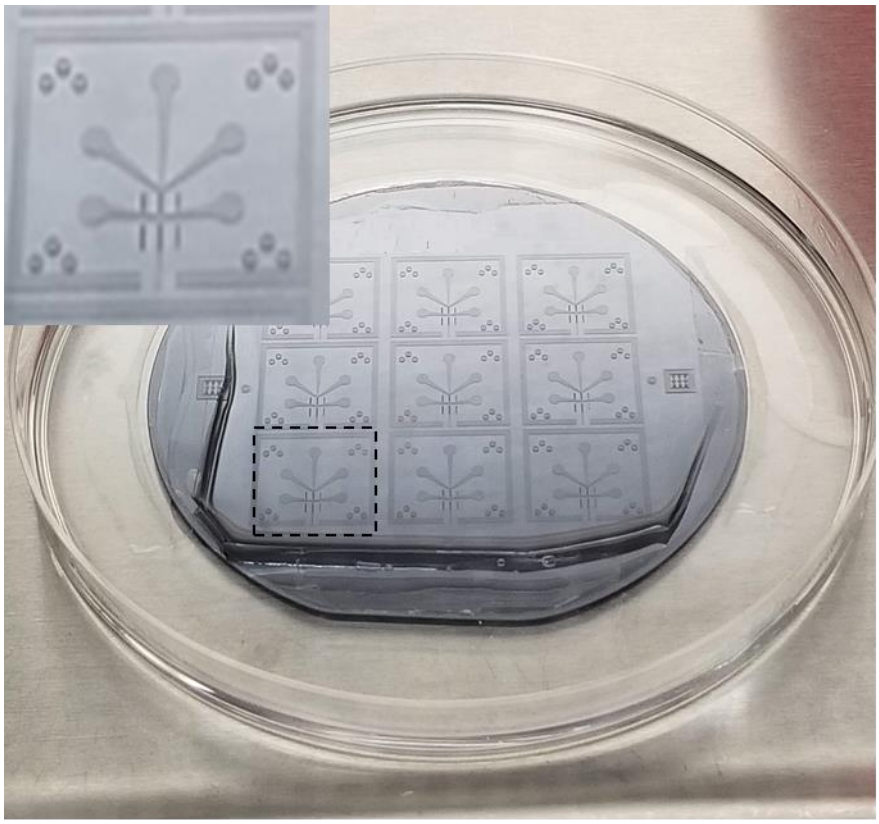

FIGURE 3: Fabricated Silicon SU-8 Wafer

The device was created using standard SU-8 techniques. The wafer was affixed to plastic petri dish and PDMS was poured over to create device. The wafer had many design

flaws. The first flaw was that the align markers and chevron geometry were on different heights. This caused adhesion issues during lithography. The second design flaw was the amount of pumps required to run the device. Since there was a 5 inlets, it mean there needed to be 5 separate syringe pumps. The third flaw was the alignment markers themselves. It proved very difficult to micro align the markers. A second wafer was created to overcome the alignment issues, but the additional activation energy supplied to the wafer caused the chevron geometry to be distorted and the device was no viable. From these flaws, a new design was created.

Wafer Design of Print Head Version Two

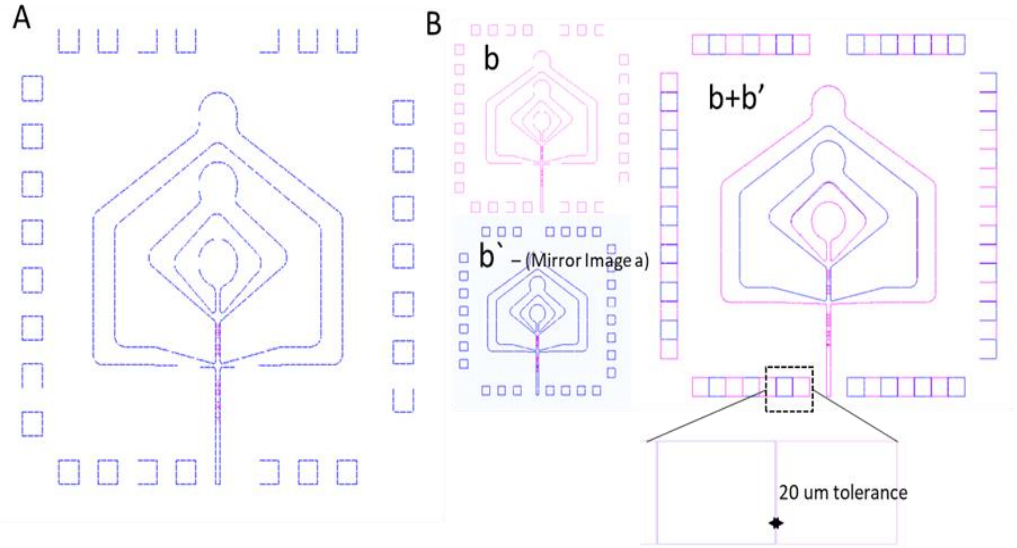

FIGURE 4: Design of Microfluidic Print Head Version 2 (a) Single device scale (b) Device mirror image. Self-alignment and tolerance view.

Taking into account the design flaws of the previous version, version 2 of the print head was created. The newly designed version has a reduction the number of inlets to limit the number of pumps required for operation. Additionally, the new design has a zipper like structure in x and y direction to semi-automatically align the device. These zippers help reduce the time and increase the accuracy of the alignment. The height issue was also fixed between the alignment markers and the chevron geometry.

Discussion

To overcome the machining limitations of coaxial printing, groups have developed microfluidic bio-printing as a way to create more physiologically relevant models[47,48,49]. Using the spatial control of microfluidic flow generators as a base[6,7,8], groups have successfully patterned many different types of fibers, including tubular[48]. The use of microfluidic print heads significantly reduce the amount of hydrogel used, reducing the price of expensive hydrogel, reagents, and number of cells. Furthermore, the direct control over cell patterning and control of extrusion speed add an extra dimension. Still the patterns created are simple including rectangle, simple sheath, or dual hemisphere[49]. Additionally, they produce large amounts of shear stress due to the low diameters.

This investigation has produced several interesting facts about the flow dynamics through a custom geometry microfluidic tip. During extrusion, the microfluidic tip is capable of 2D hydrodynamic focusing of three separate fluids. This allows to fine tune an intermediate layer that can reach 10-25 um. In addition, the micro nature of the tip allows for less use of reagents that can significantly reduce the cost of experiments. The dead volume of version two is less than 500 ul, while current tips are > 2 ml.

Additionally, the use of different geometries has shown higher uniformity. Not only does the chevron geometry successfully pattern multiple layers, it also dampens the effect of the chevrons by implementing W and WW structures. These structures create a higher amount of uniformity for the outer and intermediate sheath. Uniformity in the intermediate sheath is of special importance for the patterning of a single layer of endothelial cells. The geometry was capable of high uniformity of the intermediate sheath at outer velocity from 60 um/s to 250 um/s and intermediate velocity from 75 um/s to 150 um/s. The core was fixed at 50 um/s and showed greatest uniformity at outer sheath 30 um/s to 50 um/s and intermediate velocity of 50 um/s to 200 um/s. This range is feasible with the current syringe pumps in the lab.

The shear stress present in the tip is what is expected of the dimensions. The interesting fact is that, with expected amounts of shear from a 300 um diameter tip, the device is able to pattern a feature that is 10-25 um thick 3D feature. This is accomplished by the 2D hydrodynamic focusing and why the print head is novel. Shear stress analysis showed a safe cellular extrusion range of 50 um/s to 300 um/s for both the intermediate sheaths and outer sheaths. The core speed was fixed at 50 um/s. The cross section at critical point within the geometry showed reduce shear at the critical intermediate sheath as well as, low shear throughout the print head. This range is feasible with the current syringe pumps in the lab.

The device was created using standard SU-8 techniques. The wafer was affixed to plastic petri dish and PDMS was poured over to create device. The wafer had many design flaws. The first flaw was that the align markers and chevron geometry were on different heights. This caused adhesion issues during lithography, due to the reduced amount of polymerization energy required for successful adhesion. The second design flaw was the

amount of pumps required to run the device. Since there was a 5 inlets, it meant there needed to be 5 separate syringe pumps, which caused high amount of complexity during experiment. It also increased the overall cost of the project due to the additional need syringe pumps needed for operation. The third flaw was the alignment markers themselves. It proved very difficult to micro align the markers. This is due to the 15 um tolerance required to create a successful device and the manual movement of the device by hand, instead of using a stage to align the devices. A second wafer was created to overcome the alignment issues, but the additional activation energy supplied to the wafer caused the chevron geometry to be distorted and the device was not viable. From these flaws, a new design was created.

Taking into account the design flaws of the previous version, version two of the print head was created. The newly designed version has a reduction the number of inlets to limit the number of pumps required for operation. This was done by combining the channels of the inlets for the individual sheaths. This increased the overall size of the device by 10 mm in the Y direction. Additionally, the new design has a zipper like structure in x and y direction to semi-automatically align the device. These zippers help reduce the time and increase the accuracy of the alignment. The addition of the zipper structures allowed for alignment of the devices in the X and Y direction without the need of a fine movement stage. The zipper structures would allow for semi-automatic alignment of the device. The height issue was also fixed between the alignment markers and the chevron geometry. The issue was fixed by making a three layer chip with the chevron geometry one layer, channels on seconds, and alignment structure of third.

In future works, version two of the print head mold will be fabricated. To validate, the print head will be perfused with dyed water to show the effect of the chevron features. The new print head will be used with a suitable hydrogel to pattern a single layer of endothelial cells.

CHAPTER 3: STUDY OF HYDROGELS FOR EC MONOLAYER FORMATION

The first hydrogel to be tested will be GelMa (2%). From previous research, the 2% gel was capable of rapid gelation when exposed to ultraviolet light. It was also chosen due to lower mechanical stiffness which has been shown to reduce attachment. Additionally, the gel could be heated to 30° C to reduce viscosity.

The second hydrogel tested will be a collagen alginate blend. Due to the high concentrated of collagen needed for a successful monolayer formation, a new protocol for hydrogel synthesis must be developed.

In addition, many different hydrogel mixtures were investigated to determine a suitable one for blood brain barrier formation. The hydrogel must be capable of forming an endothelial cell monolayer with high viability. It must be cross-linkable, either ionic or ultraviolet for structural support. It must have shear thinning capabilities to be extruded at a low static pressure.

3.1 Materials and Methods

Synthesis of Collagen/Alginate Hydrogel

Alginate (biomatrix, los angeles, CA, USA) was mixed with PBS 1X (Gibco) overnight at 60C. The mixture was then cooled to 4C for more than 3 hours. The Alginate/PBS mixture was mixed with highly concentrated and neutralized collagen (Advanced BioMatrix, Boston, MA, USA) at 4C overnight to produce a 2% collagen and 1% alginate hybrid hydrogel.

Synthesis of Gel/MA Hydrogel

GelMA (biomatrix, los angeles, CA, USA) was mixed with PBS 1X (Gibco) overnight at 60C. The mixture was then cooled to 4C for more than 3 hours. The GelMA/PBS mixture was wrapped in aluminum foil.

Bio-printing Procedure

A commercially available tip (Ramehart, GA, USA) was custom ordered to affix to Cell Ink Bio-Printer (Cell-Ink). Extrusion of hybrid hydrogel was controlled via pneumatically operated valves located on bio printed. The calcium cross-linker was controlled via syringe pump (Harvard Apparatus). Endothelial cell laden hydrogel was simultaneously extruded (outer needle) with calcium chloride cross linker (center needle). The resulting lumen was extruded into media bath. The lumen was cultured until maturation (3weeks).

PI-Assay

Cell nucleus was stained via h-stain (Gibco). Propidium iodide was used to stain dead cells nucleus. Calculations of viability was determined by number of red nucleus minus blue nucleus over the number of blue nucleus.

Lypholization of Collagen

High concentrated type 1 collagen (Corning CA USA), was plated in a 6-well plate and frozen at -120° C over night. The plate was then put in a vaccuum at -150 mtorr for 1 hour.

HCMEC/D3 Culture

Immortalized brain endothelial cells were cultured using manufacturer’s media, composing of DMEM and 10% FBS, with added growth factors.

2D Hydrogel Disk Formation

All hydrogels were plated in 96 well plate. They were individually cross linked with their corresponding cross linker (UV or Ionic). Endothelial cells were plated on top of the 2D disks. For ultraviolet, the hydrogel were plated in 96 well plate and heated to 38° C to allow for a leveling of the hydrogel. The hydrogel was exposed for 30 seconds to ultraviolet lamp. For alginate/collagen mixture, hydrogel was added to the 96 well plates. Calcium chloride was added slowly top the hydrogel to insure level polymerization. After 30 seconds PBS was added to the well and was rinsed three times to rid the hydrogel of any calcium chloride that may have diffused into the 2D hydrogel construct.

3.2 Results

Attachment of Endothelial Cells to GelMa Hydrogel

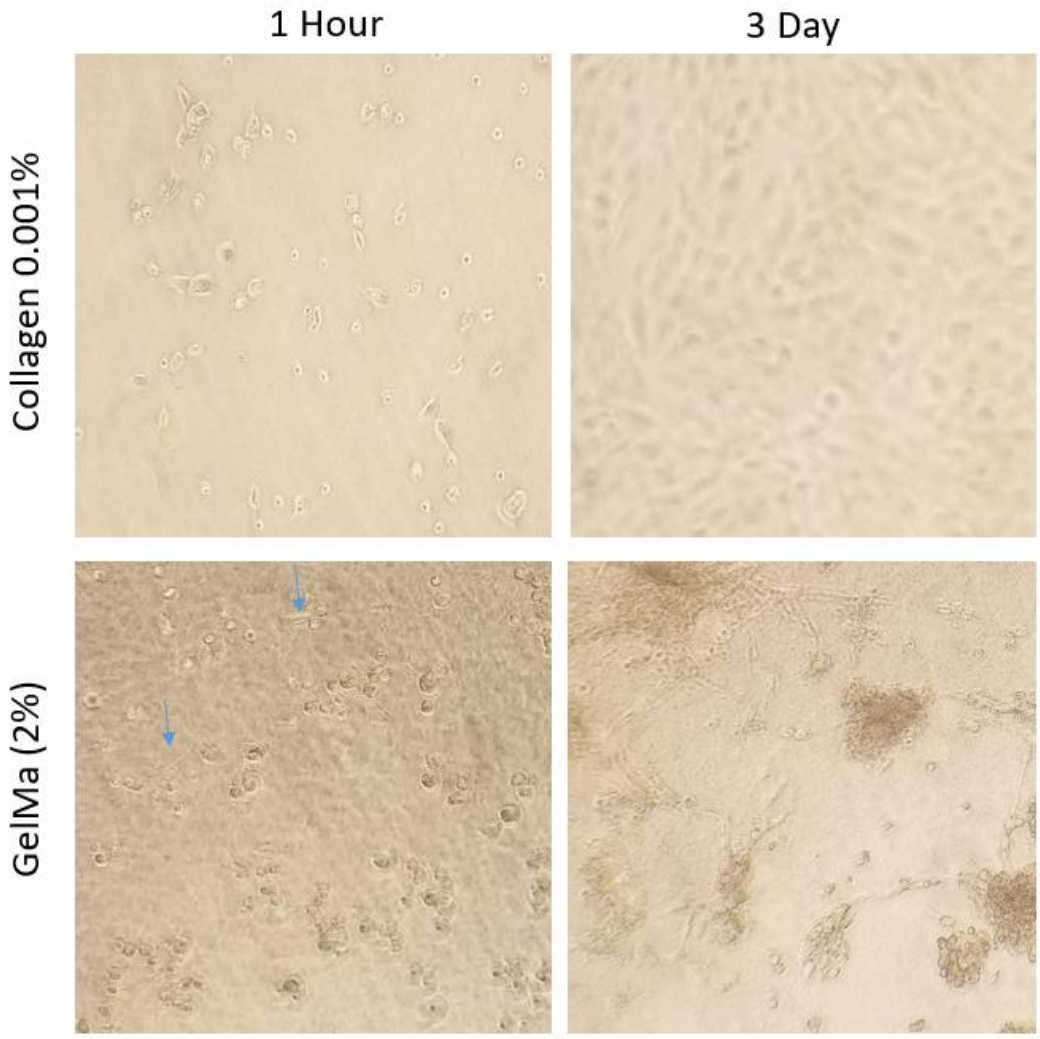

FIGURE 5: GelMa Attachment of Endothelial Cells

The hybrid GelMa hydrogel consisted of GelMa (2%). The high amount of GelMa was selected due to its rapid polymerization rate, which would be needed in the microfluidic print head. The endothelial cells showed low attachment after three days of

incubation. The lower attachment was extremely lower than the collagen control. The reduced attachment was theorized to be caused by two things, the first being a reduction in adhesive sites and the rigidness of the polymerized gelma. In order to overcome this issue, a hybrid hydrogel consisting of alginate and collagen was proposed. This was proposed due to the increase of cellular adhesion sites and the robustness of ionic crosslinking of alginate, which would provide structural support for the extruded filament.

Attachment of Endothelial Cells to Collagen/Alginate Hydrogel

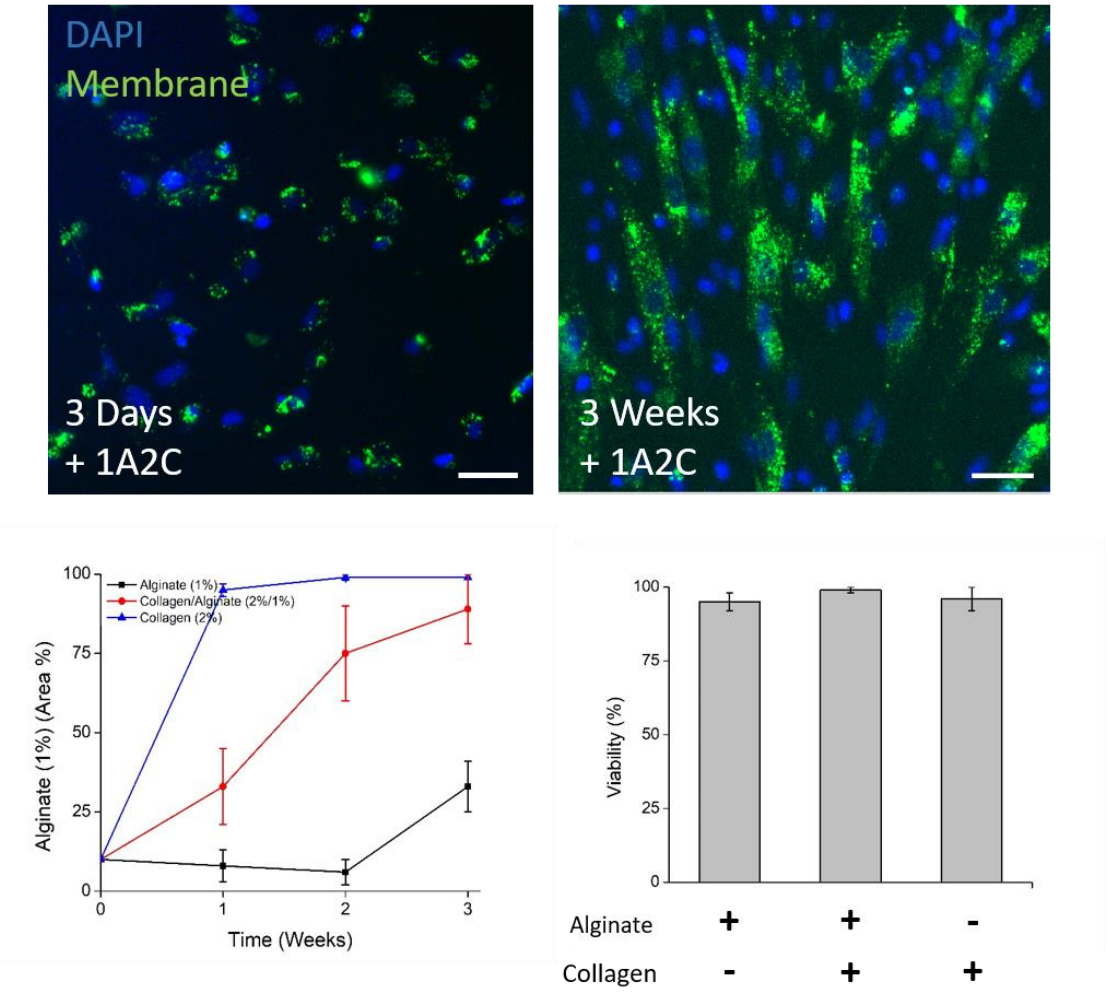

FIGURE 6: Attachment of Endothelial Cells to Hybrid Gel

The hybrid hydrogel consisted of collagen (2%) and alginate (1%). The endothelial cells showed attachment, viability, and monolayer formation. The hybrid gel showed slower monolayer formation than the collagen control, but faster than the alginate control.

Discussion

In addition to bio-printing strategies limiting the capability of a physiologically relevant neurovascular model, the relevant selection of hydrogel must also be discussed. In bio printing, hydrogels as cell delivery vehicles. Many types of cells can be viable when encapsulated within hydrogels, such as fibroblasts, chondrocytes, hepatocytes, endothelial cells, adipocytes, and stem cells[13]. During bio printing, a hydrogel with suspended cells is processed into a specifically defined shape, which is successively fixed by gelation. Gelation is usually a crosslinking reaction initiated by physical, chemical or a combination of both processes. Physical crosslinking is a reversible interaction that depends on meshes of high molecular polymer chains, ionic interactions and hydrogen bridges[14]. This type of crosslinking is compatible with biological systems such as growth factors and living cells. However, poor mechanical properties are considered as the main drawback of physical crosslinking reaction. Therefore, post processing crosslinking and/or an additional crosslinking agent is required. One example of chemical gelation by interaction between anionic groups on alginate (COO) with divalent metal ions (Ca2+). In contrast, chemical crosslinking forms new covalent bonds, which give relatively high mechanically stable constructs compared to physical crosslinking[14]. However, this type of crosslinking may involve exposure of constructs to toxic ionic solutions.

A few more examples of viable hydrogels are alginate[44], gelatin methacryloyl (GelMA)[45], and photocurable hyaluronic acid[46]. However, these hydrogels usually suffer from low cellular affinity (e.g., alginate) or strong stiffness (GelMA)[47]. Consequently, the limited cell activity impeded the development of a functional vascular model. Moreover, the lack of a platform providing consistent and tunable perfusions to the delicate hydrogel

conduits hampered the integration of mechanical and biochemical signals for biomedical applications.

In this study, GelMa and Alginate/collagen mixture was used. The hybrid hydrogel needed to be able to form an endothelial cell monolayer while having a high viability. It also needed to be cross linkable either by ultra violet or ionic cross linking. Additionally, the hydrogel needed to have shear thinning capabilities.

The first gel tested was of GelMa (2%). The 2% gel was decided on by previous experiments due to its rapid gelation when exposed to ultraviolet light. It was also chosen due to lower mechanical stiffness which has been shown to reduce attachment. Additionally, the gel could be heated to 30° C to reduce viscosity. Phosphate buffer saline and $GelMa_{80}$ (Sigma), were mixed overnight at 60 C. The warm hydrogel was then mixed with cells. The hydrogel was extruded into a 96 well plate and cross linked via UV. Cells were plated on top of hydrogel disk and allowed to incubate for 3 days. The results show that the cells had a small amount of attachment after three days. Most of the cells aggregated and did not attach. The lack of attachment was due to the lack of attachment sites or the stiffness of the cross linked hydrogel. Even though the hydrogel showed high viability, we decided to increase the number of cell adhesion sites by pursuing a second hydrogel.

The second hydrogel tested was a collagen alginate blend. First attempts of the hydrogel involved mixing alginate and highly concentrated (10mg/ml, Corning) type one collagen. Unfortunately, the acidic acid in the gel caused the alginate to fall out of solution. To fix this issue, the type one collagen underwent lyophilization, using an in house developed protocol mentioned above. The powder collagen was mixed with the

pbs/alginate mix. In practice, we found that the pH was uncontrollable due to the limited hours of vacuum time our vacuum pump could offer (1 hour). Additionally, the concentration of collagen was not high enough compared to previously published journals.

To overcome the limitations of these synthesis techniques, ultra high concentrated collagen (35 mg/ml) was purchased (Advanced Biomatrix). This collagen was neutralized and had the ability to be easily mixed with alginate/pbs (6%) mixture. After mixing the final gel had a collagen concentration of 20 mg/ml, while the alginate had a concentration of 10mg/ml. The viscosity was high, but the shear thinning effect of collagen allowed us to be confident it could be extruded. Next, hydrogel disks were formed in a 96 well plate and endothelial cells were plated on top. The disks were formed by placing 100 ul of hydrogel in the bottom and slowly adding the cross linking calcium chloride agent to the mix. After 30 seconds of crosslinking, PBS buffers was used to rinse the hydrogel disks three times. The cells attached after three days and formed a monolayer after three weeks. The delay in monolayer formation could be due to the lack of adhesive sites along the alginate part of the hydrogel. In addition, the stiffness could also be concern for cellular adhesion. The viability, showed that the hydrogel would be viable during future experiments.

In future experiments, this hydrogel could be used in unisom with the developed print head to create a high resolution blood brain barrier model for the basis of a neurovascular unit. This hydrogel met all criteria needed for the project.

REFERENCES

1. Martinez, A., Phillips, S., Whitesides, G., and Carrilho, E., (2010) "Diagnostics for the Developing World: Microfluidic Paper-Based Analytical Devices" *Analytical Chemistry* 82 (1)

2. Gravesen, P., Branebjerg, J., and Jensen, O., (1993). "Microfluidics-a review." Journal of Micromechanics and Microengineering 3(4): 168.

3. Liu, X., S. D. Carter, M. J. Renes, J. Kim, D. M. Rojas-Canales, D. Penko, C. Angus, S. Beirne, C. J. Drogemuller, Z. Yue, P. T. Coates and G. G. Wallace (2019). "Development of a Coaxial 3D Printing Platform for Biofabrication of Implantable Islet-Containing Constructs." Adv Healthc Mater 8(7): e1801181.

4. Liu, W., Z. Zhong, N. Hu, Y. Zhou, L. Maggio, A. K. Miri, A. Fragasso, X. Jin, A. Khademhosseini and Y. S. Zhang (2018). "Coaxial extrusion bioprinting of 3D microfibrous constructs with cell-favorable gelatin methacryloyl microenvironments." Biofabrication 10(2): 024102.

5. Jia, W., P. S. Gungor-Ozkerim, Y. S. Zhang, K. Yue, K. Zhu, W. Liu, Q. Pi, B. Byambaa, M. R. Dokmeci, S. R. Shin and A. Khademhosseini (2016). "Direct 3D bioprinting of perfusable vascular constructs using a blend bioink." Biomaterials 106: 58-68.

6. Eluru, G., L. A. Julius and S. S. Gorthi (2016). "Single-layer microfluidic device to realize hydrodynamic 3D flow focusing." Lab Chip 16(21): 4133-4141.

7. Langer, K., N. Bremond, L. Boitard, J. Baudry and J. Bibette (2018). "Micropipette-powered droplet based microfluidics." Biomicrofluidics 12(4): 044106.

8. Bachmann, B., S. Spitz, M. Rothbauer, C. Jordan, M. Purtscher, H. Zirath, P. Schuller, C. Eilenberger, S. F. Ali, S. Muhleder, E. Priglinger, M. Harasek, H. Redl, W. Holnthoner and P. Ertl (2018). "Engineering of three-dimensional pre-vascular networks within fibrin hydrogel constructs by microfluidic control over reciprocal cell signaling." Biomicrofluidics 12(4): 042216.

9. Thangawng, A. L., P. B. Howell, Jr., J. J. Richards, J. S. Erickson and F. S. Ligler (2009). "A simple sheath-flow microfluidic device for micro/nanomanufacturing: fabrication of hydrodynamically shaped polymer fibers." Lab Chip 9(21): 3126-3130.

10. Restrepo-Perez, L., L. Soler, C. S. Martinez-Cisneros, S. Sanchez and O. G. Schmidt (2014). "Trapping self-propelled micromotors with microfabricated chevron and heart-shaped chips." Lab Chip 14(9): 1515-1518.

11. Gao, Q., Y. He, J. Z. Fu, A. Liu and L. Ma (2015). "Coaxial nozzle-assisted 3D bioprinting with built-in microchannels for nutrients delivery." Biomaterials 61: 203-215.
12. Zhang, Y., Y. Yu, A. Akkouch, A. Dababneh, F. Dolati and I. T. Ozbolat (2015). "In Vitro Study of Directly Bioprinted Perfusable Vasculature Conduits." Biomater Sci 3(1): 134-143.

13. Lutolf, M., Gilbert, P., and Blau, H., 2009, "Designing Materials to Direct Stem-Cell Fate," Nature, 462(7272), pp. 433–441.

14. Jos, M., Jetze, V., Ferry, P., Tomasz, J., Wim, E., Wouter, J., Jürgen, G., and Dietmar, W., 2013, "25th Anniversary Article: Engineering Hydrogels for Biofabrication," Adv. Mater., 25(36), pp. 5011–5028.

15. Yang, X., Z. Lu, H. Wu, W. Li, L. Zheng and J. Zhao (2018). "Collagen-alginate as bioink for three-dimensional (3D) cell printing based cartilage tissue engineering." Mater Sci Eng C Mater Biol Appl 83: 195-201.

16. Attalla, R., E. Puersten, N. Jain and P. R. Selvaganapathy (2018). "3D bioprinting of heterogeneous bi- and tri-layered hollow channels within gel scaffolds using scalable multi-axial microfluidic extrusion nozzle." Biofabrication 11(1): 015012.

17. Benning, L., L. Gutzweiler, K. Trondle, J. Riba, R. Zengerle, P. Koltay, S. Zimmermann, G. B. Stark and G. Finkenzeller (2018). "Assessment of hydrogels for bioprinting of endothelial cells." J Biomed Mater Res A 106(4): 935-947.

18. B. Dhariwala, E. Hunt, T. Boland Rapid prototyping of tissue-engineering constructs, using photopolymerizable hydrogels and stereolithography Tissue Eng., 10 (9–10) (2004), pp. 1316-1322

19. D.R. Albrecht, G.H. Underhill, T.B. Wassermann, R.L. Sah, S.N. Bhatia Probing the role of multicellular organization in three-dimensional microenvironments Nat. Methods, 3 (5) (2006), pp. 369-375

20. T. Boland, T. Xu, B. Damon, X. Cui Application of inkjet printing to tissue engineering Biotechnol. J., 1 (9) (2006), pp. 910-917

21. T. Boland, V. Mironov, A. Gutowska, E.A. Roth, R.R. Markwald Cell and organ printing 2: fusion of cell aggregates in three-dimensional gels Anat. Rec. A Discov. Mol. Cell. Evol. Biol., 272 (2) (2003), pp. 497-502

22. T. Xu, J. Jin, C. Gregory, J.J. Hickman, T. Boland Inkjet printing of viable mammalian cells Biomaterials, 26 (1) (2005), pp. 93-99

23. Xu, C.A. Gregory, P. Molnar, X. Cui, S. Jalota, S.B. Bhaduri, T. Boland

Viability and electrophysiology of neural cell structures generated by the inkjet printing method Biomaterials, 27 (19) (2006), pp. 3580-3588

24. J.A. Barron, P. Wu, H.D. Ladouceur, B.R. Ringeisen Biological laser printing: a novel technique for creating heterogeneous 3-dimensional cell patterns Biomed. Microdevices, 6 (2) (2004), pp. 139-147

25. B.R. Ringeisen, H. Kim, J.A. Barron, D.B. Krizman, D.B. Chrisey, S. Jackman, R.Y. Auyeung, B.J. Spargo Laser printing of pluripotent embryonal carcinoma cells Tissue Eng., 10 (3–4) (2004), pp. 483-491

26. N.R. Schiele, D.T. Corr, Y. Huang, N.A. Raof, Y. Xie, D.B. Chrisey Laser-based direct-write techniques for cell printing Biofabrication, 2 (3) (2010), p. 032001

27. J. Yan, Y. Huang, D.B. ChriseyLaser-assisted printing of alginate long tubes and annular constructs Biofabrication, 5 (1) (2013), p. 015002

28. S. Khalil, W. Sun Biopolymer deposition for freeform fabrication of hydrogel tissue constructs Mater. Sci. Eng. C, 27 (3) (2007), pp. 469-478

29. Y. Yan, Z. Xiong, Y. Hu, S. Wang, R. Zhang, C. Zhang Layered manufacturing of tissue engineering scaffolds via multi-nozzle deposition Mater. Lett., 57 (18) (2003), pp. 2623-2628

30. B. Duan, L.A. Hockaday, K.H. Kang, J.T. Butcher 3D bioprinting of heterogeneous aortic valve conduits with alginate/gelatin hydrogels J. Biomed. Mater. Res. A, 101 (5) (2013), pp. 1255-1264

31. S. Ghorbanian, M.A. Qasaimeh, M. Akbari, A. Tamayol, D. Juncker Microfluidic direct writer with integrated declogging mechanism for fabricating cell-laden hydrogel constructs Biomed. Microdevices, 16 (3) (2014), pp. 387-395

32. S.T. Beyer, A. Bsoul, A. Ahmadi, K. Walus 3D Alginate Constructs for Tissue Engineering Printed Using a Coaxial Flow Focusing Microfluidic Device (2013), pp. 1206-1209

33. V. Mironov, V. Kasyanov, C. Drake, R.R. Markwald Organ printing: promises and challenges Regen. Med., 3 (1) (2008), pp. 93-103

34. M. Nakamura, S. Iwanaga, C. Henmi, K. Arai, Y. Nishiyama Biomatrices and biomaterials for future developments of bioprinting and biofabrication Biofabrication, 2 (1) (2010), p. 014110

35. X. Ji, Z. Su, P. Wang, G. Ma, S. Zhang “Ready-to-use” hollow nanofiber membrane-based glucose testing strips Analyst, 139 (24) (2014), pp. 6467-6473

36. Y. Zhang, Y. Yu, H. Chen, I.T. Ozbolat Characterization of printable cellular micro-fluidic channels for tissue engineering Biofabrication, 5 (2) (2013), p. 025004

37. Y. Zhang, Y. Yu, A. Akkouch, A. Dababneh, F. Dolati, I.T. Ozbolat In vitro study of directly bioprinted perfusable vasculature conduits Biomater. Sci., 3 (1) (2014), pp. 134-143

38. F. Dolati, Y. Yu, Y. Zhang, A.M. De Jesus, E.A. Sander, I.T. Ozbolat In vitro evaluation of carbon-nanotube-reinforced bioprintable vascular conduits Nanotechnology, 25 (14) (2014), p. 145101

39. Y. Yu, Y. Zhang, J.A. Martin, I.T. Ozbolat Evaluation of cell viability and functionality in vessel-like bioprintable cell-laden tubular channels J. Biomech. Eng., 135 (9) (2013), p. 91011

40. I.T. Ozbolat, H. Chen, Y. Yu Development of 'Multi-arm Bioprinter' for hybrid biofabrication of tissue engineering constructs Robot. Comput. Integ. Manuf., 30 (3) (2014), pp. 295-304

41. V. Mironov, R.P. Visconti, V. Kasyanov, G. Forgacs, C.J. Drake, R.R. Markwald Organ printing: tissue spheroids as building blocks Biomaterials, 30 (12) (2009), pp. 2164-2174

42. F. Pati, J. Jang, D.-H. Ha, S. W. Kim, J.-W. Rhie, J.-H. Shim, D.-H. Kim, D.-W. Cho, *Nat. Commun.* 2014, **5**, 3935.

43. J. Jang, J. Y. Park, G. Gao, D.-W. Cho, *Biomaterials* 2018, **156**, 88.

44. Q. Gao, Y. He, J.-Z. Fu, A. Liu, L. Ma, *Biomaterials* 2015, **61**, 203;

45. W. Jia, P. S. Gungor-Ozkerim, Y. S. Zhang, K. Yue, K. Zhu, W. Liu, Q. Pi, B. Byambaa, M. R. Dokmeci, S. R. Shin, *Biomaterials* 2016, **106**, 58.

46. L. Ouyang, C. B. Highley, W. Sun, J. A. Burdick, *Adv. Mater*. 2017, **29**, 1604983.

47. W. Liu, Z. Zhong, N. Hu, Y. Zhou, L. Maggio, A. K. Miri, A. Fragasso, X. Jin, A. Khademhosseini, Y. S. Zhang, *Biofabrication* 2018, **10**, 024102.

48. Pi, Q., S. Maharjan, X. Yan, X. Liu, B. Singh, A. M. van Genderen, F. Robledo-Padilla, R. Parra-Saldivar, N. Hu, W. Jia, C. Xu, J. Kang, S. Hassan, H. Cheng, X. Hou, A. Khademhosseini and Y. S. Zhang (2018). "Digitally Tunable Microfluidic Bioprinting of Multilayered Cannular Tissues." Adv Mater 30(43): e1706913.

49. Liu, H., H. Zhou, H. Lan, F. Liu and X. Wang (2018). "Multinozzle Multichannel Temperature Deposition System for Construction of a Blood Vessel." SLAS Technol 23(1): 64-69.

50. Costantini, M., J. Idaszek, K. Szoke, J. Jaroszewicz, M. Dentini, A. Barbetta, J. E. Brinchmann and W. Swieszkowski (2016). "3D bioprinting of BM-MSCs-loaded ECM biomimetic hydrogels for in vitro neocartilage formation." Biofabrication 8(3).